Article

Ion-Induced Nucleation *in Solution*: Promotion of Solute Nucleation in Charged Levitated Droplets

Neil D. Draper, Samuel F. Bakhoum, Allen E. Haddrell, and George R. Agnes

J. Am. Chem. Soc., **2007**, 129 (37), 11364-11377• DOI: 10.1021/ja067094i • Publication Date (Web): 24 August 2007

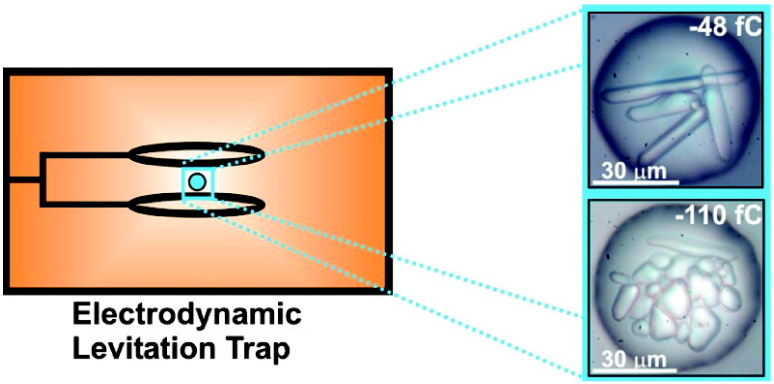

More About This Article

Additional resources and features associated with this article are available within the HTML version:

- Supporting Information
- Access to high resolution figures
- Links to articles and content related to this article
- Copyright permission to reproduce figures and/or text from this article

View the Full Text HTML

J|A|C|S
ARTICLES
Published on Web 08/24/2007

Ion-Induced Nucleation *in Solution*: Promotion of Solute Nucleation in Charged Levitated Droplets

Neil D. Draper, Samuel F. Bakhoum, Allen E. Haddrell, and George R. Agnes*

Contribution from the Department of Chemistry, Simon Fraser University, Burnaby, BC, V5A 1S6, Canada

Received October 3, 2006; E-mail: gagnes@sfu.ca

Abstract: We have investigated the nucleation and growth of sodium chloride in both single quiescent charged droplets and charged droplet populations that were levitated in an electrodynamic levitation trap (EDLT). In both cases, the magnitude of a droplet's net excess charge ($ions_{DNEC}$) influenced NaCl nucleation and growth, albeit in different capacities. We have termed the phenomenon ion-induced nucleation *in solution*. For single quiescent levitated droplets, an increase in $ions_{DNEC}$ resulted in a significant promotion of NaCl nucleation, as determined by the number of crystals observed. For levitated droplet populations, a change in NaCl crystal habit, from regular cubic shapes to dome-shaped dendrites, was observed once a surface charge density threshold of -9×10^{-4} e·nm^{-2} was surpassed. Although promotion of NaCl nucleation was observed for droplet population experiments, this can be attributed in part to the increased rate of solvent evaporation observed for levitated droplet populations having a high net charge. Promotion of nucleation was also observed for two organic acids, 2,4,6-trihydroxyacetophenone monohydrate (THAP) and α-cyano-4-hydroxycinnamic acid (CHCA). These results are of direct relevance to processes that occur in both soft-ionization techniques for mass spectrometry and to a variety of industrial processes. To this end, we have demonstrated the use of ion-induced nucleation *in solution* to form ammonium nitrate particles from levitated droplets to be used in *in vitro* toxicology studies of ambient particle types.

Introduction

The nucleation of crystals from solution is a phenomenon of widespread importance with many biological, environmental, atmospheric, and industrial implications. The desired, distinct physiochemical properties of a chemical material can be obtained by controlling crystallite preparation.[1−3] For example, different crystalline forms of a drug can vary in solubility, absorption, and stability properties.[4−6] As such, control of the crystallization process is one of the most valuable techniques used in separation and purification processes employed by a variety of industries, including not only pharmaceuticals but agrochemicals, pigments, foods, and explosives.[2,7−9]

However, solute nucleation from a supersaturated solution is a complex operation. Similar to a chemical reaction, it is an activated process with a transition state. Unlike the formation of covalent bonds and a transition state molecular complex for a chemical reaction, a cluster composed of a few tens of molecules, held together by weak intermolecular forces and packed in some regular arrangement, is considered the transition state for nucleation.[2]

From a mechanistic point of view, solute nucleation is a two-step process: a result derived from the bulk diffusion of growth units through a mass transfer boundary layer and their subsequent incorporation into the growing crystal lattice.[1,2,10,11] Although both steps are governed by different mechanisms, they are both influenced by experimental variables such as temperature, solvent evaporation rate, solution stirring rate, the addition of nucleation agents and stabilizers, and the influence of magnetic[12−14] and electric fields.[15−17] Changes in the experimental variables result in changes to the rates of nucleation and crystal growth, which influence changes in crystal habit and morphology.

The effect of an external electric field on nucleation kinetics and crystal growth in saturated solutions was first investigated by both Shubnikov and Kozlovskii, who determined that

(1) Lacmann, R.; Herden, A.; Mayer, C. *Chem. Eng. Technol.* **1999**, *22*, 279−289.
(2) Davey, R.; Garside, J. *From Molecules to Crystallizers: An Introduction to Crystallization*; Oxford University Press: Oxford, 2000.
(3) Piana, S.; Reyhani, M.; Gale, J. D. *Nature* **2005**, *438*, 70−73.
(4) Gavezzotti, A.; Filippini, G. *J. Am. Chem. Soc.* **1995**, *117*, 12299−12305.
(5) Ni, X. W.; Valentine, A.; Liao, A. T.; Sermage, S. B. C.; Thomson, G. B.; Roberts, K. J. *Cryst. Growth Des.* **2004**, *4*, 1129−1135.
(6) Sun, X. Y.; Garetz, B. A.; Myerson, A. S. *Cryst. Growth Des.* **2006**, *6*, 684−689.
(7) Bernstein, J. *J. Phys. D Appl. Phys.* **1993**, *26*, B66−B76.
(8) Bernstein, J. *Chem Commun.* **2005**, 5007−5012.
(9) Aber, J. E.; Arnold, S.; Garetz, B. A.; Myerson, A. S. *Phys. Rev. Lett.* **2005**, *94*, (145503)145501−145504.
(10) Brice, J. C. *Crystal Growth Processes*; Blackie & Son Ltd: Glasgow, 1986.
(11) Garside, J.; Mersmann, A.; Nâyvlt, J.; Institution of Chemical Engineers; European Federation of Chemical Engineering. Working Party on Crystallization. *Measurement of Crystal Growth and Nucleation Rates*, 2nd ed.; Institution of Chemical Engineers: Rugby, U.K., 2002.
(12) Furukawa, Y.; Nomura, K.; Katagiri, C.; Matsuura, Y.; Mogi, I. *Nippon Kessho Seicho Gakkaishi* **2004**, *31*, 280.
(13) Micheletto, R.; Matsui, J.; Oyama, M.; El-Hami, K.; Matsushige, K.; Kawakami, Y. *Appl. Surf. Sci.* **2005**, *242*, 129−133.
(14) Saban, K. V.; Jini, T.; Varghese, G. *Cryst. Res. Technol.* **2005**, *40*, 748−751.
(15) Koch, C. C. *Mater. Sci. Eng. A-Struct.* **2000**, *287*, 213−218.
(16) Sahin, O. *Cryst. Res. Technol.* **2002**, *37*, 183−192.
(17) Tang, J. C.; Li, S. D.; Mao, X. Y.; Du, Y. W. *J. Phys. D Appl. Phys.* **2005**, *38*, 729−732.

10.1021/ja067094i CCC: $37.00

nucleation rates of ammonium chloride and ammonium bromide increased in the presence of an external electric field.[18−20] Recently, electric field strengths of greater than 10^5 V·m^{-1} were also shown to have significant controlling effects on $PbCO_3$ and NaCl nucleation.[21−23] Although several reports confirm that externally applied electric fields have a stimulating effect on the nucleation rate of small molecule crystals in saturated solutions,[23,24] a significant decrease in the number of nuclei was observed when an external electric field was used for the crystallization of the protein lysozyme.[25,26] As such, the lysozyme crystals obtained were fewer in number, larger in size, and of better crystallographic quality as quantified by a reduction in their mosaic spread upon X-ray diffraction;[25−28] a most important goal for crystallogenesis studies on biological macromolecules.[29,30] This contrasting result certainly suggests that more research is necessary to better understand the mechanism of nucleation and crystal growth in the presence of electric fields. Unfortunately, there are only a few theoretical considerations concerning this problem;[23,24,31−35] most of them related to processes that occur in Wilson cloud chambers.

Wilson was the first person to quantitatively investigate ion-induced nucleation,[36,37] which has been defined as the promotion of cluster growth around an ion which acts as a heterogeneous nucleus for the condensation of supersaturated vapors.[38−40] The strong ion-dipole interaction between ions and vapor molecules lowers the activation barrier and hence reduces the supersaturation necessary for nucleation.[40] In the microelectronics industry, it has been shown that gaseous C^- reduces the critical cluster radius required for nucleation and that the net charge of the resulting cluster promotes further growth of the nucleus during the low-pressure synthesis of diamonds.[41,42] Nucleation rates of silicone particles, via the condensation of neutral silicone vapor on Si^- in processing plasmas, have also been modeled using ion-induced nucleation theory.[43] Moreover, the phenomenon of ion-induced nucleation has important implications with regards to atmospheric processes, where ions provide condensation sites for sulfuric acid and water vapors to form new aerosol particles that can grow into sizes needed for cloud condensation nuclei and ice nuclei. This in turn affects the particle size distribution and lifetimes of clouds and hence the radiative properties that factor into atmospheric albedo forcing climate change.[44−49]

Although the physics of droplets that possess net charge is a subject that continues to receive attention, the condensed phase chemistry occurring within such droplets, as a result of the net charge localized in the diffuse layer at the droplet−air interface, is not well characterized.[50−53] Mass spectrometry studies of cluster ions released from charged droplets in an electrospray have identified shifts in chemical equilibria[54,55] and the formation of preferred nanocrystalline structures.[56−61] It has also been observed by Pruppacher that sulfur particles, which typically act as poor ice nuclei at −20 °C, are able to cause ice formation in supercooled droplets at −8 °C when they are electrified.[44,62] This charge-enhanced contact nucleation is usually described as field-induced electrofreezing, the process whereby an electric field causes the freezing of a supercooled water drop.[44,63−67] Thus, there could be a wealth of knowledge regarding the chemistry that occurs in charged droplets as a result of their violation of electroneutrality.[51,52]

In our previous electrodynamic levitation studies with charged droplets, we have reported the enhancement of α-cyano-4-hydroxycinnamic acid (CHCA) cocrystallization with one or more peptides[51] and the promotion of NaCl precipitation,[52] both a function of the magnitude of the droplet's net charge. This phenomenon of promoted solute nucleation was termed ion-induced nucleation *in solution* and has several implications for laboratory, industrial, and natural processes involving media with net charge ranging from fundamental aspects of soft ionization for mass spectrometry[68,69] to the preparation of

(18) Shubnikov, A. V.; Parvov, V. F. *Kristallografiya* **1961**, *6*, 443−450.
(19) Kozlovskii, M. I. *Kristallografiya* **1962**, *7*, 157−159.
(20) Kozlovskii, M. I. *Krist. Fazovye Perekhody, Otd. Fiz. Tverd. Tela i Poluprov., Akad. Nauk Belorussk. SSR* **1962**, 404−410.
(21) Pillai, K. M.; Vaidyan, V. K.; Ittyachan, M. A. *Cryst. Res. Technol.* **1981**, *16*, K82−K84.
(22) Saban, K. V.; Thomas, J.; Varghese, G. *Indian J. Phys. A* **2002**, *76A*, 355−359.
(23) Saban, K. V.; Thomas, J.; Varughese, P. A.; Varghese, G. *Cryst. Res. Technol.* **2002**, *37*, 1188−1199.
(24) Saban, K. V.; Varghese, G. *Indian J. Pure Ap. Phy.* **2002**, *40*, 552−555.
(25) Taleb, M.; Didierjean, C.; Jelsch, C.; Mangeot, J. P.; Capelle, B.; Aubry, A. *J. Cryst. Growth* **1999**, *200*, 575−582.
(26) Taleb, M.; Didierjean, C.; Jelsch, C.; Mangeot, J. P.; Aubry, A. *J. Cryst. Growth* **2001**, *232*, 250−255.
(27) Charron, C.; Didierjean, C.; Mangeot, J. P.; Aubry, A. *J. Appl. Crystallogr.* **2003**, *36*, 1482−1483.
(28) Nanev, C. N.; Penkova, A. *J. Cryst. Growth* **2001**, *232*, 285−293.
(29) Fourme, R.; Ducruix, A.; Rieskautt, M.; Capelle, B. *J. Synchrotron Radiat.* **1995**, *2*, 136−142.
(30) Fourme, R.; Ducruix, A.; Ries-Kautt, M.; Capelle, B. *J. Cryst. Growth* **1999**, *196*, 535−545.
(31) Kashchiev, D. *J. Cryst. Growth* **1972**, *13*, 128−130.
(32) Kashchiev, D. *Philos. Mag.* **1972**, *25*, 459−470.
(33) Dhanasekaran, R.; Ramasamy, P. *J. Cryst. Growth* **1986**, *79*, 993−996.
(34) Cheng, K. J. *Phys. Lett. A* **1984**, *106*, 403−404.
(35) Isard, J. O. *Philos. Mag. (1798−1977)* **1977**, *35*, 817−819.
(36) Wilson, C. T. R. *Philos. T. R. Soc. Lond. A* **1899**, *192*, 403−455.
(37) Wilson, C. T. R. *Philos. T. R. Soc. Lond. A* **1899**, *123*, 289−308.
(38) Castleman, A. W.; Holland, P. M.; Keesee, R. G. *J. Chem. Phys.* **1978**, *68*, 1760−1767.
(39) De, B. R. *J. Chem. Phys.* **1979**, *70*, 2046−2047.
(40) Gamero-Castano, M.; de la Mora, J. F. *J. Chem. Phys.* **2002**, *117*, 3345−3353.
(41) Jang, H. M.; Hwang, N. M. *J. Mater. Res.* **1998**, *13*, 3527−3535.
(42) Jang, H. M.; Hwang, N. M. *J. Mater. Res.* **1998**, *13*, 3536−3549.
(43) Girshick, S. L.; Rao, N. P.; Kelkar, M. *J. Vac. Sci. Technol. A* **1996**, *14*, 529−534.
(44) Harrison, R. G. *Space Sci. Rev.* **2000**, *94*, 381−396.
(45) Lee, S. H.; Reeves, J. M.; Wilson, J. C.; Hunton, D. E.; Viggiano, A. A.; Miller, T. M.; Ballenthin, J. O.; Lait, L. R. *Science* **2003**, *301*, 1886−1889.
(46) Lovejoy, E. R.; Curtius, J.; Froyd, K. D. *J. Geophys. Res.-Atmos.* **2004**, *109*, D08204.
(47) Wilhelm, S.; Eichkorn, S.; Wiedner, D.; Pirjola, L.; Arnold, F. *Atmos. Environ.* **2004**, *38*, 1735−1744.
(48) Bazilevskaya, G. A.; Krainev, M. B.; Makhmutov, V. S. *J. Atmos. Sol.-Terr. Phys.* **2000**, *62*, 1577−1586.
(49) Tabazadeh, A.; Djikaev, Y. S.; Reiss, H. *Proc. Natl. Acad. Sci. U.S.A.* **2002**, *99*, 15873−15878.
(50) Haddrell, A. E.; Agnes, G. R. *Anal. Chem.* **2004**, *76*, 53−61.
(51) Bogan, M. J.; Bakhoum, S. F. W.; Agnes, G. R. *J. Am. Soc. Mass Spectrosc.* **2005**, *16*, 254−262.
(52) Bakhoum, S. F. W.; Agnes, G. R. *Anal. Chem.* **2005**, *77*, 3189−3197.
(53) Myland, J. C.; Oldham, K. B. *J. Electroanal. Chem.* **2002**, *522*, 115−123.
(54) Wang, H. J.; Agnes, G. R. *Anal. Chem.* **1999**, *71*, 4166−4172.
(55) Wang, H. J.; Agnes, G. R. *Anal. Chem.* **1999**, *71*, 3785−3792.
(56) Thomson, B. A. *J. Am. Soc. Mass Spectrosc.* **1997**, *8*, 1053−1058.
(57) Hao, C. Y.; March, R. E.; Croley, T. R.; Smith, J. C.; Rafferty, S. P. *J. Mass Spectrom.* **2001**, *36*, 79−96.
(58) Hao, C. Y.; March, R. E. *J. Mass Spectrom.* **2001**, *36*, 509−521.
(59) Counterman, A. E.; Clemmer, D. E. *J. Phys. Chem. B* **2001**, *105*, 8092−8096.
(60) Julian, R. R.; Hodyss, R.; Kinnear, B.; Jarrold, M. F.; Beauchamp, J. L. *J. Phys. Chem. B* **2002**, *106*, 1219−1228.
(61) Takats, Z.; Nanita, S. C.; Cooks, R. G. *Angew. Chem., Int. Ed.* **2003**, *42*, 3521−3523.
(62) Pruppacher, H. R. *Pure Appl. Geophys.* **1973**, *104*, 623−634.
(63) Harrison, R. G. *Atmos. Environ.* **1997**, *31*, 3483−3484.
(64) Tripathi, S. N.; Harrison, R. G. *Atmos. Res.* **2002**, *62*, 57−70.
(65) Braslavsky, I.; Lipson, S. G. *Appl. Phys. Lett.* **1998**, *72*, 264−266.
(66) Svishchev, I. M.; Kusalik, P. G. *Phys. Rev. B* **1996**, *53*, R8815−R8817.
(67) Svishchev, I. M.; Kusalik, P. G. *J. Am. Chem. Soc.* **1996**, *118*, 649−654.
(68) Fenn, J. B.; Mann, M.; Meng, C. K.; Wong, S. F.; Whitehouse, C. M. *Science* **1989**, *246*, 64−71.
(69) Karas, M.; Hillenkamp, F. *Anal. Chem.* **1988**, *60*, 2299−2301.

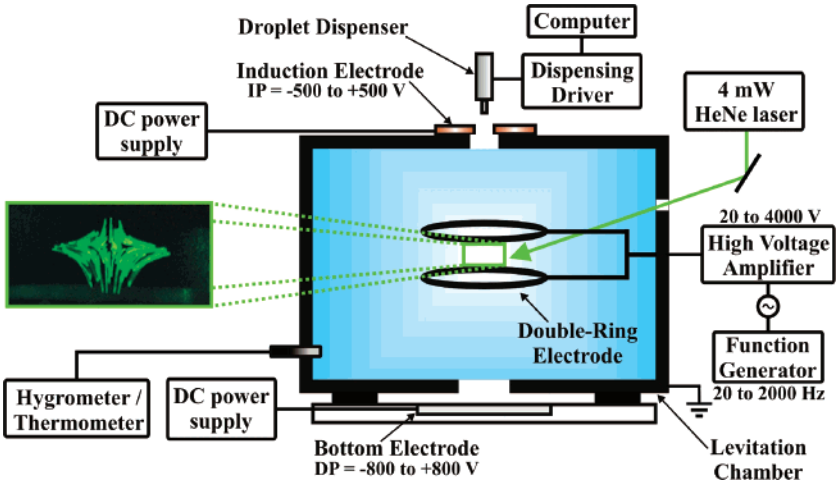

Figure 1. Schematic of the electrodynamic levitation trap (EDLT) showing the important operational components. The inset is a representative image of laser light scattered by a population of droplets levitated in the EDLT.

nanophase materials with improved properties.[70,71] Preliminary characterization of its threshold behavior is described in this paper. Furthermore, a method that uses ion-induced nucleation *in solution* to prepare ammonium nitrate particles that are subsequently used in *in vitro* toxicology studies of ambient particle types has been developed. We anticipate that this type of heterogeneous nucleation in charged levitated droplets will be of use to investigators whose areas of application interest span materials science through to biochemistry.

Experimental Section

The apparatus for levitation of droplets is depicted in Figure 1. The steps involved in the methodology used to dispense and characterize these droplets, and the droplets that are levitated for time periods between 30 s to several hours, are described below.

Chemicals. Reagent grade NaCl, methanol, and glycerol were purchased from BDH. The 20 nm FluoSpheres used, purchased from Molecular Probes (Invitrogen Inc., Burlington, ON, Canada), are polystyrene-based spheres (density = 1.05 g mL^{-1}) that encapsulate ~180 fluorescein molecules per sphere. They are supplied as suspensions (2% solids) in water. Ammonium nitrate (NH_4NO_3), 2,4,6-trihydroxyacetophenone monohydrate (THAP), and α-cyano-4-hydroxycinnamic acid (CHCA) were purchased from Aldrich. All aqueous solutions were prepared using distilled water (dH_2O).

Dispensing of Droplets with Net Charge. A micropipette was used to load a 3 μL aliquot of a starting solution into the reservoir of an inkjet-style droplet dispenser (models MJ-AB-01-40 and MJ-AB-01-60, Microfab Technologies Inc., Plano, TX). Activation of the piezoceramic crystal bonded to the outside of the dispenser's reservoir generated an acoustic wave that caused a volume of liquid to pass through the nozzle as a jet that then separates from the nozzle and subsequently collapses to form a monodisperse droplet. The nozzle of the dispenser was positioned over a 5.0 mm diameter hole cut into a flat copper electrode. A dc potential applied to this electrode using a high voltage power supply (model PS350, Stanford Research Systems, Sunnyvale, CA) established an electric field between it and the nozzle, influencing ion mobility in the jet prior to its separation from the dispenser nozzle. This induced charge separation within the jet caused the resultant droplet to have a net excess charge.[52] Variation of the dc potential applied to the induction electrode proportionally varied the magnitude of the image charge imparted onto the droplets. Each of these droplets then passed into an electrodynamic levitation trap (EDLT) where they were trapped and levitated.

Measurement of Initial Volume Dispensed and Droplet Net Charge. The initial volume of a droplet was determined using fluorescence emission microscopy. After loading a dispenser (40 μm diameter orifice) reservoir with an aqueous solution of FluoSpheres (50 μL of FluoSpheres in 25 mL of dH_2O), a predetermined number of droplets were dispensed consecutively onto a glass coverslip where they dried forming a small spot. Droplets were dispensed using a 10 V waveform amplitude applied to the droplet dispenser at a frequency of 1 Hz. A series of these spots made up of differing numbers of droplets were deposited in a row on the same coverslip, and the fluorescence emission of each spot was measured. An optical microscope (Zeiss Axioplan 2, Motic, North York, ON) fitted with an excitation filter (BP-546/12) and emission filter (LP-590) was used to collect all images of fluorescence emission. For each sample spot, fluorescence emission was collected from a 1.50 mm × 2.00 mm area centered over the site of droplet deposition. The signal intensity of the fluorescence emission for each image was determined using Image J software (Research Services Branch, National Institute of Mental Health, Bethesda, MD) and integrated. The resultant calibration graph of fluorescence emission signal intensity vs number of droplets is shown in Figure 2A. The fluorescence emission from a known volume ($V = 0.020 \pm 0.005$ μL) of the same aqueous solution, as deposited by microliter syringe onto a glass coverslip, was then measured under identical conditions as those employed for the fluorescence emission measurement of the spots. By using the calibration graph, the initial dispensed droplet volume was calculated to be 250 ± 90 pL (average radius = 39 ± 14 μm) for a 40 μm diameter orifice dispenser. It should be noted that different droplet dispenser waveform amplitudes and frequencies result in different dispensed droplet volumes.

The induced droplet net charge was determined by dispensing individual charged droplets directly onto a metal target plate connected to an electrometer (model 6517a, Keithley Instruments, Cleveland, OH). For these measurements of droplet net charge magnitude, the droplet dispenser, induction electrode, and metal target plate were situated inside a Faraday cage. The separation distance between the nozzle tip and the induction electrode was 1.25 ± 0.02 mm while the separation distance between the induction electrode and metal target plate was ~40 mm. The magnitude of the induced net charge per droplet was plotted as a function of the dc potential applied to the induction electrode (Figure 2B).

Data points for dispensed droplets were the average of 100 droplets dispensed using the same 10 V waveform amplitude applied to the droplet dispenser at a frequency of 1 Hz. The polarity of the

(70) Nakaso, K.; Han, B.; Ahn, K. H.; Choi, M.; Okuyama, K. *J. Aerosol Sci.* **2003**, *34*, 869−881.
(71) Suh, J.; Han, B.; Kim, D. S.; Choi, M. *J. Aerosol Sci.* **2005**, *36*, 1183−1193.

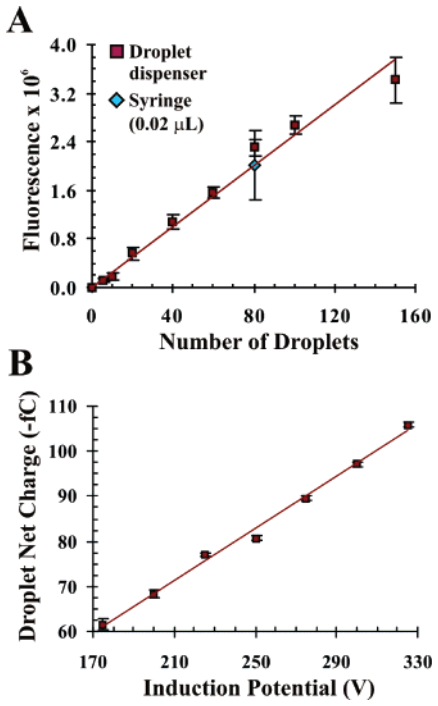

Figure 2. (A) Calibration of the initial volume of droplets dispensed using the fluorescence emission from FluoSpheres against volumes delivered by a micropipette. (B) Measurement of the net excess charge on dispensed droplets as a function of induction potential.

charge induced on the forming droplet is opposite to the polarity of the dc potential applied to the induction electrode. The magnitude of the dc potential did not affect the volume of the droplet dispensed within experimental error as determined using fluorescence emission microscopy.

Droplet Levitation Apparatus. The electrodynamic levitation trap (EDLT) used in this study (Figure 1) has been previously described.[72,73] Its two ring electrodes were constructed using single stranded 1 mm diameter copper wire that were each shaped into 2 cm diameter rings and mounted parallel to each other at a separation distance of approximately 6 mm. The pair of rings was positioned between two flat end-cap electrodes referred to as the induction and the bottom electrode. The induction electrode during droplet dispensing also served as the upper end-cap electrode for the EDLT during droplet levitation.[74] Typically, the dc electric field between it and the lower end-cap flat electrode is used to balance the force of gravity acting on the droplets. However, the nonhyperbolic electrode shape and positioning used in the EDLT resulted in significant deviations from a quadrupole electric field, which permitted ongoing droplet levitation after the potentials of both the upper and lower end cap electrodes had both been reduced to 0 V while maintaining a sine wave on the ring electrodes. It should be noted that two EDLTs were used in the course of this study: one for droplet population experiments, whereby a 60 Hz sine wave, 500−2700 $V_{O-P,}$ was applied to both rings, in phase, by use of an in-house constructed Variac-controlled voltage amplifier, and one for single droplet experiments, whereby a sine wave (50−700 Hz, ±500−4000 V) was applied to both rings, produced using a function generator (model TFG-4613, Topward Electric Instruments Co., Taipei Hsien, Taiwan) in series with a high voltage variable frequency amplifier (model 609E-6, Trek Inc., Medina, NY). Immediately after a droplet was trapped in single droplet experiments, the ac frequency applied to the rings was increased from ∼80 Hz to ∼700 Hz, in order to ensure it was quiescent. By reducing the ac potential of the ring electrodes, while both the upper and lower end cap electrodes were held at 0 V, the force of gravity exerted on the charged droplet caused it to fall out of the ac trap and to be deposited on the lower end-cap electrode, or target plate, at the end of each levitation experiment. This deposition procedure was strictly adhered to for singly levitated charged droplet experiments. The distance between the center of the ring electrodes and the deposition plate was 15 mm. All electrode potentials were relative to ground potential (0 V). The droplets in the EDLTs were illuminated via forward scattering by a 4 mW green (λ = 543 nm) HeNe laser (Uniphase model 1676, Manteca, CA) that was defocused (laser spot size diameter ∼6 mm). Although laser light can affect nucleation from solution,[75] several control experiments were conducted, confirming that nucleation was unaffected by the HeNe laser.

Characterization of Droplet Residues. Each experiment involved flushing the internal reservoir of the droplet dispenser with clean solvent and then filling it with a 3 μL volume of a starting solution. Starting solutions were composed of zero or one solute in a solvent mixture of water/glycerol, unless otherwise noted. Within 2−5 s of the droplet dispensing event, the majority of the volatile solvents evaporated, leaving behind a droplet composed of glycerol and the nonvolatile solutes, referred to throughout this manuscript as the droplet residue. In most experiments, a glass coverslip was positioned on top of the bottom electrode of the EDLT where the droplet residues were eventually deposited at the end of each levitation experiment. Droplet residues were characterized by optical microscopy (model B5 Professional, Motic, Richmond, BC).

Effect of Droplet Mobility on the Rate of Solvent Evaporation. The trajectories of multiple droplets simultaneously levitated in the EDLT (see Figure 1 inset) depend on several factors such as the geometry of the ring electrodes and the potentials applied to them, droplet mass, droplet net charge, and the number of droplets simultaneously levitated. For dispensed droplets of the same volume, an increase in droplet net charge may result in higher droplet mobility for a droplet population trapped at atmospheric pressure during levitation in an EDLT. Results from single droplet studies have demonstrated a substantial enhancement in the evaporation rate for stably oscillating single droplets over their stationary droplet counterparts.[76,77] Hence, a population of charged droplets having a higher droplet mobility should experience enhancement of the droplet evaporation rate relative to a population of charged droplets having a lower droplet mobility. The effect of droplet mobility on the rate of solvent evaporation over the range of conditions used in this study was first determined before preliminary characterization of ion-induced nucleation *in solution* took place.

A population of droplets was dispensed from a water/glycerol starting solution (99:1 v/v) using a 10 V waveform amplitude applied to the droplet dispenser (40 μm diameter orifice) at a frequency of 1 Hz. The dc potential applied to the induction electrode was kept constant for the dispensing of each droplet in a population that was levitated in the EDLT. The relative humidity and temperature of the chamber was monitored with a digital humidity meter (model L914797, VWR International, Edmonton, AB). Over the course of this and all subsequent experiments, the temperature and relative humidity of the EDLT chamber had average values of 22 ± 1 °C and 33 ± 5%, respectively, unless otherwise noted.

The evaporation of solvent from each droplet levitated leads to Coulomb instability of the droplet at a size that can be calculated[78,79]

(72) Bogan, M. J.; Agnes, G. R. *Anal. Chem.* **2002**, *74*, 489−496.
(73) Bogan, M. J.; Agnes, G. R. *J. Am. Soc. Mass Spectrosc.* **2004**, *15*, 486−495.
(74) Davis, E. J.; Buehler, M. F.; Ward, T. L. *Rev. Sci. Instrum.* **1990**, *61*, 1281−1288.
(75) Garetz, B. A.; Matic, J.; Myerson, A. S. *Phys. Rev. Lett.* **2002**, *89*, 175501, 175501−175504.
(76) Zhu, J. H.; Zheng, F.; Laucks, M. L.; Davis, E. J. *J. Colloid Interface Sci.* **2002**, *249*, 351−358.
(77) Guan, G. Q.; Zhu, J. H.; Xia, S. L.; Feng, Z. H.; Davis, E. J. *Int. J. Heat Mass Trans.* **2005**, *48*, 1705−1715.
(78) Rayleigh, L. *Philos. Mag. (1798−1977)* **1882**, *14*, 184−186.
(79) Smith, J. N.; Flagan, R. C.; Beauchamp, J. L. *J. Phys. Chem. A* **2002**, *106*, 9957−9967.

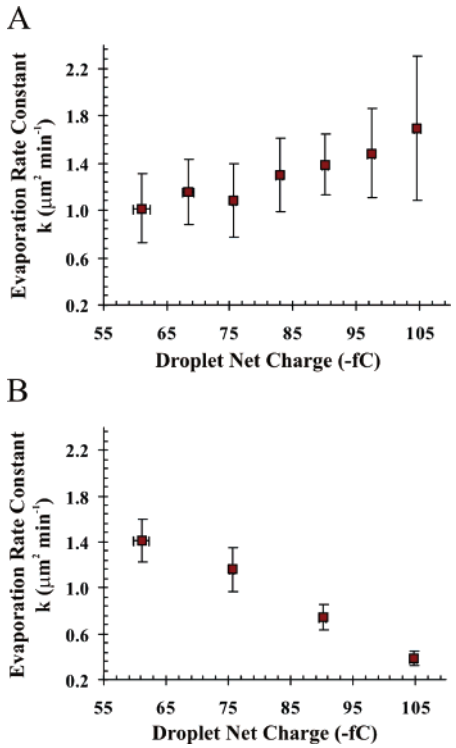

Figure 3. (A) Evaporation rate constant of levitated droplet residue populations as a function of their net excess charge. (B) Evaporation rate constant of single quiescent levitated droplet residues as a function of their net excess charge.

resulting in the eventual loss of the droplet from the EDLT following a Coulomb explosion event. The size at which a levitated droplet first undergoes Coulomb explosion can be estimated based on its physical and chemical description at the start of an experiment along with the Coulomb explosion relationship:[80]

$$Q^2 < 64\pi^2\gamma\epsilon_o r^3 \quad (1)$$

which relates the stability of the droplet as a function of its surface tension (γ) and its radius (r) to the magnitude of its net elementary charge (Q). Forces resulting from the surface tension stabilize droplet shape while the electrostatic forces resulting from the net excess charges destabilize the droplet. It is assumed that the decrease in droplet diameter as a function of time is given by the so-called d^2-law:[80]

$$d_C^2 = d_o^2 - kt \quad (2)$$

where d_C is the calculated droplet residue diameter at the Coulomb explosion limit, d_o is the initial droplet residue diameter following volatile solvent evaporation, k is the evaporation rate constant, and t is the time required for a droplet in a population to undergo Coulomb explosion as indicated by the loss of the droplet from the EDLT. The experiment was repeated for several droplet populations using different induction electrode potentials while keeping the population number constant. It should be noted that during the course of each experiment, the amplitude of the ac field in the EDLT was periodically adjusted in order to maintain the droplet trajectories constant. The results are plotted in Figure 3A.

The average evaporation rate constant increased in a linear fashion from 1.0 ± 0.3 μm^2 min^{-1} for droplets having -61.1 ± 1.3 fC net charge to 1.7 ± 0.6 μm^2 min^{-1} for droplets having -104.7 ± 0.5 fC net charge. An application of the *t*-test to the droplet population having the lowest net charge with the population having the highest net charge ($t = 4.65$; degrees of freedom $= 42$; $P < 0.0001$) demonstrated that these two mean values of k were significantly different. Hence, the population of droplets with higher mobility (i.e., droplets having higher net charge) evaporated more quickly than the droplet population having lower mobility (i.e., droplets having lower net charge) as previously suggested. The calculated k values of the glycerol droplet residues were significantly greater than those reported by Ray et al. for single, quiescent glycerol droplets in humid air streams ($k = 0.26$, 0.31 μm^2 min^{-1} for % RH = 30, 40, respectively).[81]

The same type of experiment was then repeated for single, quiescent levitated droplets in lieu of a population. Using the same droplet dispenser settings as described above, a single droplet was dispensed and then trapped and levitated quiescently until its eventual loss from the EDLT following a Coulomb explosion event. The experiment was repeated many times using four different induction electrode potentials, and the results were plotted in Figure 3B.

The evaporation rate constant decreased from 1.4 ± 0.2 μm^2 min^{-1} to 0.4 ± 0.1 μm^2 min^{-1} as the droplet net charge was increased from -61.1 ± 1.3 fC to -104.7 ± 0.5 fC. An application of the *t*-test to the data set for individual droplets having the lowest net charge with the data set for individual droplets having the highest net charge ($t = 21.83$; degrees of freedom $= 37$; $P < 0.0001$) demonstrated that these two mean values of k were significantly different. Unexpectedly, not only were the four calculated k values significantly greater than those reported by Ray et al. for single glycerol droplets, the observed decrease in k for increasing droplet net charge was also in violation of the d^2-law, which Ray reported as being strictly adhered to for single glycerol droplets at a given relative humidity.[81] A third odd finding was that for the same droplet net charge of -61.1 ± 1.3 fC, the k value for a quiescent droplet (1.4 ± 0.2 μm^2 min^{-1}) was significantly greater than the corresponding droplet population k value (1.0 ± 0.3 μm^2 min^{-1}). It was likely that droplet−droplet interactions were responsible for the observed decrease in k value for droplets levitated in a population vs single levitated droplets. Experimental investigations performed on simple multidroplet configurations have demonstrated that the rate of droplet evaporation decreases as the number of droplets in the population increases and that the decrease in k was dependent upon the interdrop spacing.[82] It was assumed that no droplet−droplet collisions occur since each droplet in a population had the same polarity and magnitude of net elementary charge.

The observed decrease for k, as shown in Figure 3B, was not likely a direct function of the droplet's net excess charge. In his work with the electrostatic application of pesticide sprays, Law demonstrated that the electric charge on evaporating liquid droplets neither altered k nor was dissipated by evaporation for water droplets in humid air.[83] However, the presence of surface charge does alter the phase equilibrium between a droplet and the surrounding vapor. For the above experiments, the origin of the ions that comprise the net excess charge of the droplet ($ions_{DNEC}$) was either various impurities present in the solvents used, or arrived at via electrolysis.[84] Modeling studies of such droplets suggest that $ions_{DNEC}$ are localized in a diffuse layer at the droplet−air interface where they collectively form an electric potential that diminishes to null in the center of the droplet.[53] The equilibrium solvent vapor pressure is modified by the chemical activity of the $ions_{DNEC}$ which lowers the solvent vapor pressure.[85] This effect can lead to large supersaturations in small liquid droplets. The correction to the vapor pressure over a droplet due to the surface charge is given by:[86]

$$\ln(p/p_o) = [-2Q^2M(\epsilon - 1)]/[\pi\rho RTd^4] \quad (3)$$

(80) Frohn, A.; Roth, N. *Dynamics of Droplets*; Springer: Berlin, 2000.

(81) Ray, A. K.; Johnson, R. D.; Souyri, A. *Langmuir* **1989**, *5*, 133−140.
(82) Tian, Y. R.; Apfel, R. E. *J. Aerosol Sci.* **1996**, *27*, 721−737.
(83) Law, S. E. *IEEE Trans. Ind. Appl.* **1989**, *25*, 1081−1087.
(84) VanBerkel, G. J.; Zhou, F. M.; Aronson, J. T. *Int. J. Mass Spectrom. Ion Processes* **1997**, *162*, 55−67.

where p and p_o are the vapor pressures over the droplet in presence and absence of surface charge, respectively, M is the molecular weight of the liquid, ϵ is the dielectric constant of the solution, ρ is the solution density, R is the gas constant, and T is the absolute temperature. For the glycerol droplet residue diameters ($d \sim 10$ μm) and elementary net charges ($Q \sim 3-7 \times 10^5$) used in this study, the surface charge was predicted to have a negligible effect on the vapor pressure above the droplet.

In several experiments involving single droplets, the Davis group have shown that evaporating single component droplets followed the d^2-law until the droplets fissioned at approximately 90% of the theoretical Rayleigh limit of charge, whereby a small mass loss, along with a large charge loss, occurred during a Coulomb explosion event.[87−89] Perhaps the observed decrease in k may have been due to the droplet residues undergoing Coulomb explosion several times prior to the parent droplet loss from the EDLT. Droplets having higher initial levels of net charge would probably be more susceptible to this possibility. If multiple Coulomb explosion events had occurred, then t was overestimated, resulting in artificially low k values for droplets with higher net charge, accounting for the lack of adherence to the d^2-law. It should be noted that a droplet can be destabilized by an external electric field, whereby an instability is induced leading to a discharge event.[89] The critical field at which this occurs is known as the Taylor limit given by the following:

$$E_c^{\,2} = c[\gamma/4\pi\epsilon_o r] \tag{4}$$

where c is a fitting constant whose accepted value is ~2.64 for liquid droplets in air.[90,91] The electric fields the glycerol droplet residues ($r \sim 5$ μm) encountered in the EDLT were several orders of magnitude smaller than the critical field ($E_c \sim 1.7 \times 10^7$ V·m^{-1}) necessary to cause their premature fission.

On the other hand, if we were to assume that the single droplets having low net charge were not, in fact, completely quiescent due to small translations and/or rotations present that were not distinguished, and that as the droplet net charge was increased, these small translations and/or rotations of the droplets were reduced, then the discrepancies between the magnitude of the k values calculated and the apparent deviation to the d^2-law may both be accounted for. Deviations from a quadruple electric field in the ac trap, as introduced by the nonhyperbolic shape and positioning of the electrodes used in the EDLT, would give credence to such an explanation. Nonetheless, more sophisticated light-scattering techniques such as optical resonance spectroscopy[87,88] would be necessary to further study the kinetics of droplet evaporation as presented here.

Results and Discussion

NaCl Nucleation and Growth in Levitated Droplets Having Net Charge. Recently, we presented evidence that control of the magnitude of the net charge (i.e., ions$_{DNEC}$) contained in a levitated droplet can be used to promote the cocrystallization of an organic acid, α-cyano-4-hydroxycinnamic acid (CHCA), with one or more peptides.[51] It is widely believed that indiscriminate cocrystallization of compounds having a wide range of properties within a host compound is a necessary requirement for optimal preparation of solid samples for matrix-assisted laser desorption ionization (MALDI) mass spectrometry (MS).[92,93] To characterize the role of ions$_{DNEC}$ (i.e., droplet net charge) in affecting crystal nucleation and growth, a series of experiments were performed to elucidate the effect of relevant and readily varied properties of levitated droplets. These experiments involving droplets having net charge were designed so that droplets would not undergo Coulomb explosion.

The effect of droplet net charge on NaCl nucleation was determined. For the following two trials, a calibrated 40 μm diameter orifice droplet dispenser with a 10 V applied waveform at 1 Hz was used to dispense droplets from a 298 mM NaCl aqueous starting solution containing 571 mM glycerol (water:glycerol = 97:3 v/v). NaCl was chosen as the nucleating solute because of the relative simplicity of the system and the certainty with which the identity of the ions$_{DNEC}$ that constitute the droplet net charge could be assigned, Cl^- ions$_{DNEC}$ or Na^+ ions$_{DNEC}$ depending on the polarity of the induction electrode.[52]

The first trial was composed of several experiments, whereby single droplets were dispensed, trapped, and levitated. Each droplet had a net charge of ~−48 fC (induction potential (IP) = 130 V). Within ~5 s of droplet formation, the volume of each levitated droplet decreased significantly, because of the rapid evaporation of H_2O, until equilibrium with the levitation chamber was reached. Since the chamber was kept at a relative humidity (% RH) of 0−5%, the droplet residue volume shrank to ~7.5 pL (average radius ~12.1 μm) and became saturated in NaCl (NaCl solubility in glycerol = 1.711 M).[94] After 5 min of levitation, the quiescent droplet residue was deposited onto a glass coverslip and the number of individual NaCl crystals formed was counted. Previously described control experiments have demonstrated that NaCl precipitation occurred in the levitated residues and not as a result of heterogeneous nucleation at the glass slide−residue interface.[52] The crystals obtained had regular cubic habits and the length of a side of each crystal in the droplet residue was measured in order to ascertain the size of each salt crystal. Numerous repeat experiments were conducted.

The second trial was composed of several experiments conducted under the same conditions as the first trial, with the exception of net droplet charge which was increased to ~−110 fC (IP = 330 V). The total number of NaCl crystals was counted, and the side length for each crystal in the droplet residue was measured. Numerous repeat experiments were conducted. The results were plotted as histograms, as shown by the three representative data sets in Figure 4. Each histogram consisted only of the data collected during one particular day since day-to-day differences in both room temperature and % RH (outside the levitation chamber where analysis of the droplet residues took place) were significant. All three histograms demonstrated that the size distribution of NaCl crystals was affected by the net charge of the droplet. For droplet residues that had −48 fC net charge, the distribution of NaCl crystals that had side lengths <2.5 μm were 6.2, 2.4, and 10.5%, respectively, while the distribution of NaCl crystals that had side lengths ≥4.0 μm were 45.1, 42.9, and 36.5%, respectively.

(85) Friedlander, S. K. *Smoke, Dust, and Haze: Fundamentals of Aerosol Behavior*; Wiley: New York, 1977.
(86) Cohen, M. D.; Flagan, R. C.; Seinfeld, J. H. *J. Phys. Chem.* **1987**, *91*, 4563−4574.
(87) Taflin, D. C.; Zhang, S. H.; Allen, T.; Davis, E. J. *AIChE J.* **1988**, *34*, 1310−1320.
(88) Taflin, D. C.; Ward, T. L.; Davis, E. J. *Langmuir* **1989**, *5*, 376−384.
(89) Davis, E. J.; Bridges, M. A. *J. Aerosol Sci.* **1994**, *25*, 1179−1199.
(90) Grimm, R. L.; Beauchamp, J. L. *J. Phys. Chem. B* **2003**, *107*, 14161−14163.
(91) Grimm, R. L.; Beauchamp, J. L. *J. Phys. Chem. B* **2005**, *109*, 8244−8250.
(92) Kahr, B.; Gurney, R. W. *Chem. Rev.* **2001**, *101*, 893−951.
(93) Gluckmann, M.; Pfenninger, A.; Kruger, R.; Thierolf, M.; Karas, M.; Horneffer, V.; Hillenkamp, F.; Strupat, K. *Int. J. Mass Spectrom.* **2001**, *210*, 121−132.
(94) Stecher, P. G. *The Merck Index: An Encyclopedia of Chemicals and Drugs*, 8th ed.; Merck: Rahway, NJ, 1968.

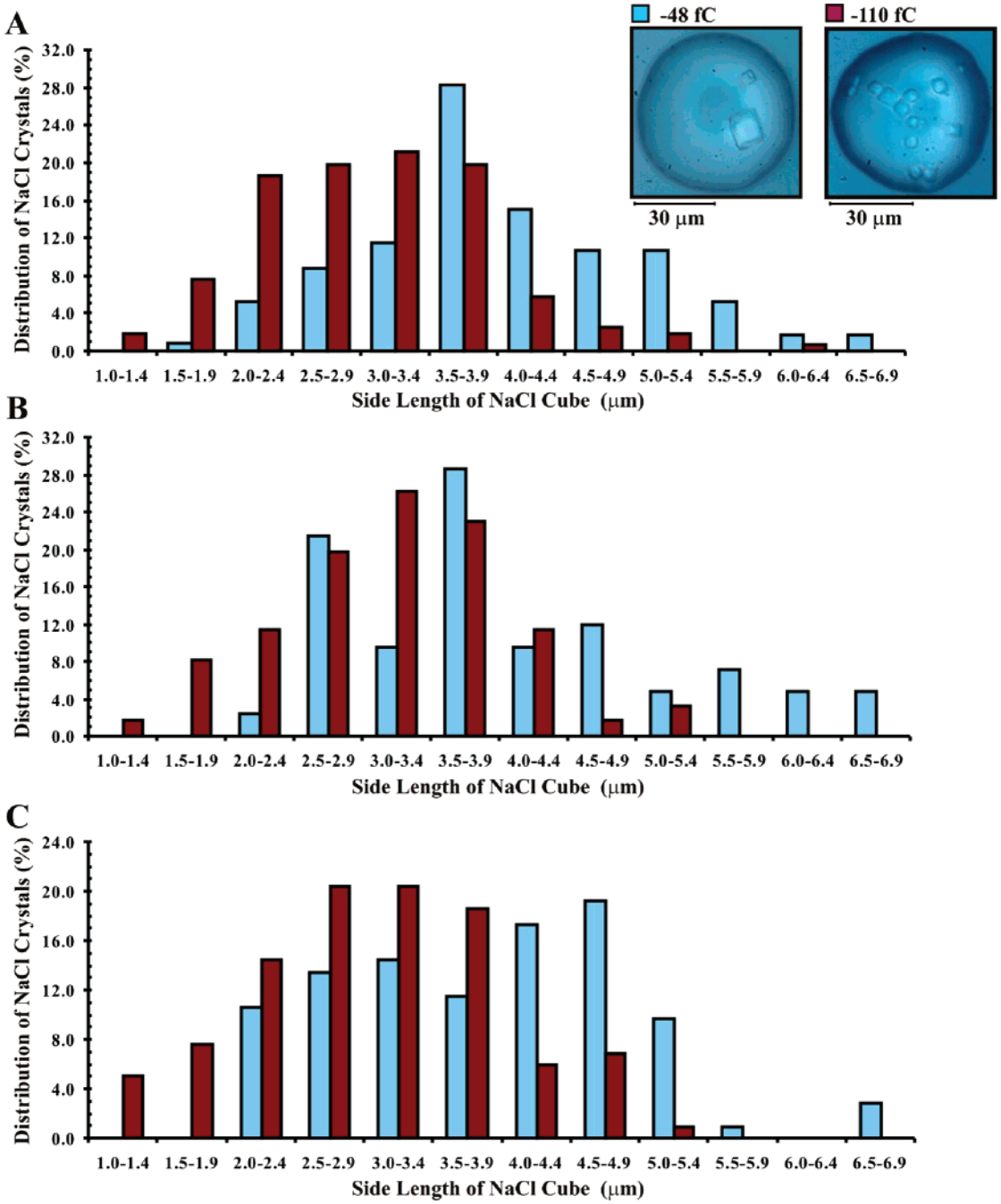

Figure 4. Size distribution of NaCl crystals observed in single quiescent droplet residues having a net excess charges of −48 fC (blue color) or −110 fC (red color), respectively over the course of 1 day. (A) Data collected on May 31, 2006; ambient % RH = 30. (B) Data collected on June 8, 2006; ambient % RH = 36. (C) Data collected on June 19th, 2006; ambient % RH = 38. The two insets are representative images of NaCl crystals that had formed in single quiescent droplet residues having a net excess charge of −48 fC (left) or −110 fC (right), respectively.

This distribution shifted toward smaller crystal size as the droplet residue net charge increased to −110 fC (side length <2.5 μm : 28.2, 21.3, and 27.0%, respectively; side length ≥4.0 μm : 10.9, 16.4, and 13.5%, respectively). Examination of the data also showed that the average number of crystals per droplet was always slightly higher for droplets having higher net charge (−48 fC : number of crystals/droplet = 14.1, 6.0, and 11.6, respectively; −110 fC : number of crystals/droplet = 19.5, 8.7, and 13.1, respectively).

This result suggested that increasing the magnitude of droplet net charge resulted in a promotion of solute nucleation for a given initial droplet residue NaCl concentration. It was likely that the increase in the number of nuclei present for droplets having higher net charge was responsible for the observed decrease in crystal size as a result of increased competition for solute molecules.

According to classical nucleation theory, the driving force for nucleation and growth of crystals from solution is the supersaturation ($\Delta\mu$) which is commonly expressed as follows:[95]

$$\Delta\mu = \mu_s - \mu_c = kT \ln S \tag{5}$$

where μ_s and μ_c are the chemical potentials of a molecule in solution and in the bulk of the crystal phase, respectively, k is

the Boltzmann constant, T is the absolute temperature, and S is the supersaturation ratio which is defined as:[95]

$$S = [a_1 \cdot a_2 \cdot ... \cdot a_j]/[a_{1e} \cdot a_{2e} \cdot ... \cdot a_{je}] \quad (6)$$

where a_1, a_2, ..., a_j and a_{1e}, a_{2e}, ..., a_{je} are the actual and equilibrium values of the different ions in solution that come together to make up an crystal, respectively. For non-ionic crystals this reduces to:

$$S = a/a_e \quad (7)$$

Nucleation and growth of crystals is only possible when the solution is supersaturated (i.e., $\Delta\mu > 0$ and $S > 1$).

The work (W) to form a cluster of $n = 1, 2, 3,...$ molecules (or ion pairs) is typically described by two contributions, one from the decreased free energy due to the formation of the cluster and the other due to the interfacial energy between the forming cluster and the solution. For a spherical cluster that assembles in the volume of a solution consisting only of solvent and solute (i.e., homogeneous nucleation), W can be written as follows:[95]

$$W = -nkT \ln S + (36\pi {\nu_o}^2)^{1/3} \gamma_i n^{2/3} \quad (8)$$

where n is the number of molecules (or ion pairs) in the cluster, ν_o is the volume occupied by a molecule (or ion pair) in the cluster, and γ_i is the surface energy of the interface between solution and cluster. The critical cluster size is that for which W is maximized with respect to n; once the cluster has reached this size, it can grow spontaneously into a crystal. The critical size n^* and the subsequent energy barrier W^* to nucleation is given by:[95]

$$n^* = 32\pi {\nu_o}^2 {\gamma_i}^3/3(kT)^3 \ln^3 S \quad (9)$$

$$W^* = 16\pi {\nu_o}^2 {\gamma_i}^3/3(kT)^2 \ln^2 S \quad (10)$$

whereby both n^* and W^* are decreasing functions of S. The rate of nucleation J can then be expressed as:

$$J = A \exp[-W^*/kT] \quad (11)$$

where A is a pre-exponential factor.

For these experiments, we have speculated that the origins of the ions that comprise the ions$_{DNEC}$ are derived from the NaCl electrolyte added to the starting solution. Even though the residues contained a total of $\sim 4.5 \times 10^{13}$ dissolved ions, the influence of $\sim 7 \times 10^5$ Cl^- ions$_{DNEC}$ in droplet residues having -110 fC of net charge could have influenced the nucleation process since nucleation involves only a small number of atoms,[96] and that these ions$_{DNEC}$ could have enhanced ordering in the diffuse layer at the droplet−air interface. A sufficiently high supersaturation of Cl^- or Na^+, depending on droplet net charge polarity, in such a layer could create a driving force for nucleation and growth of $NaCl_{(s)}$.[95] However, it is difficult to believe that such a minute difference in S between droplets having -110 fC and -48 fC could result in the observed promotion in NaCl nucleation.

From eqs 10 and 11, it is clear that J depends strongly on the interfacial energy term γ_i, whereby small changes in this parameter can lead to large changes in the nucleation rate. It is unclear whether or not γ_i is affected by the droplet residue's net charge. Molecular dynamic simulations are currently underway to investigate this scenario.

Perhaps the interaction of the ions$_{DNEC}$ in the electric field of the EDLT influenced the observed promotion in nucleation. Charged solute clusters that have not yet become fully crystalline in the supersaturated solution could be aligned by the electric field, causing an organization of the clusters and moving them along the path to crystallization.[9] Furthermore, the migration of ions, as influenced by the electric field, would alter local supersaturations at the droplet−air interface which, in turn, could influence nucleation. The free energy required for the formation of a crystalline cluster in the presence of an external electric field can be written as:[22−24]

$$W = -nkT \ln S + (36\pi {\nu_o}^2)^{1/3} \gamma_i n^{2/3} + \Delta G_E \quad (12)$$

where ΔG_E is the change in electrostatic energy when n ion pairs transform from solution to the cluster in the presence of the electric field. Investigations have shown that the electric field stimulates nucleation when the dielectric constant of the cluster is less than dielectric constant of the solution.[22−24]

The observations of promoted NaCl nucleation as affected by droplet net charge (i.e., ion-induced nucleation *in solution*) are similar to those of Saban et al., whereby the application of an external electric field enhanced the NaCl nucleation rate in large neutral droplets placed in a parallel plate capacitor. The number of observed NaCl crystals increased while the average NaCl crystal size decreased above an electric field threshold of 2×10^5 V·m^{-1}, especially for lower S values.[22] Although in our studies, by comparison, the charged droplet residues experienced a dynamic electric field in the EDLT, we speculated that the influence of the ions$_{DNEC}$ had a greater influence on the observed solute nucleation since both trials were conducted using the same EDLT parameters with the exception of droplet net excess charge. If one assumed the quiescent levitated droplet residues are spherical and that the ions$_{DNEC}$ were localized in a diffuse layer at the residue−air interface, then the electric field at the residue surface due to ions$_{DNEC}$ can be estimated. For droplets having -48 fC and -110 fC of net charge, $E \sim 2.5 \times 10^6$ V·m^{-1} and 5.7×10^6 V·m^{-1}, respectively, values larger than the 2×10^5 V·m^{-1} required to influence NaCl nucleation rates as reported by Saban et al., assuming that NaCl nucleation occurred at the residue interface. On account of Gauss's Law, the electric field inside the droplet would be 0 V·m^{-1}. Work is underway to observe even larger differences between droplets having a greater range of net charge.

Another possible explanation for the observed increase in crystal number for droplet residues of higher net charge is as follows: Since evaporation of the solvent from the droplet creates a gradient in solute concentration that is at a maximum at the droplet−air interface,[97,98] we speculate that nucleation likely occurred at or near the droplet residue surface. It is also likely then that the critical clusters incorporated charge, as the ions$_{DNEC}$ are mainly located in the diffuse layer at the droplet−

(95) Kashchiev, D.; van Rosmalen, G. M. *Cryst. Res. Technol.* **2003**, *38*, 555−574.
(96) Cohen, M. D.; Flagan, R. C.; Seinfeld, J. H. *J. Phys. Chem.* **1987**, *91*, 4583−4590.
(97) Ford, I. J. *Mater. Res. Soc. Symp. Proc.* **1996**, *398*, 637−642.
(98) Leong, K. H. *J. Aerosol Sci.* **1987**, *18*, 525.

air interface. If we were to assume that each growing crystal must be charged, and assuming that the total amount of material crystallized was approximately constant between droplet residues having low and high net charge (as observed by an increase in crystal number with a decrease in crystal size for residues having high net charge when compared to residues of low net charge), then, because of reduced like-charge repulsion, a system of many smaller and lesser charged crystals is probably more thermodynamically stable than a system of fewer, larger, and higher charged crystals. In other words, the droplet residues having higher net charge reduces Ostwald ripening of the crystals rather than altering the nucleation rate *J*.

It should be noted that in their investigations of electrodynamically levitated water droplets, Krämer et al., found that small variations in the magnitude of droplet net charge did not affect the nucleation of ice for 60 μm diameter droplets carrying a maximum of $\pm$ 0.37 pC (surface charge density value = $\pm$ 2.04×10^{-4} e•nm^{-2}).[99] Although the surface charge density values were comparable to the maximum used in these single quiescent droplet NaCl nucleation trials ($\pm 3.14 \times 10^{-4}$ e•nm^{-2}), the nucleating species (H_2O vs NaCl) and system (nucleation from the melt vs nucleation from solution) were different. However, the ice nucleation rates for Krämer's electrodynamically levitated charged droplets were larger than those measured in cloud chamber studies, suggesting that the crystallization process was affected by either the ions$_{DNEC}$, the electric field of the EDLT, or both factors.[49] Notwithstanding, there is theoretical evidence that a strong dc electric field can induce H_2O crystallization. Molecular dynamics simulations by Svishchev et al. showed that supercooled water can be induced to crystallize by a dc field of magnitude 5×10^9 V•m^{-1}.[100] Similar simulations of supercooled water in the absence of a field have yielded crystallization only once.[101]

The effect of droplet net charge on NaCl nucleation was also investigated with populations of droplets. In these trials, the number of NaCl crystals observed to have formed in the residues of a population of droplets that had a high net charge (−325 fC) was typically twice that observed in the residues of droplets that had a low net charge (−135 fC). The observed increase in crystal number for the population trials can be attributed, in part, to the increased rate of solvent evaporation observed for a population of droplets having a high net charge. This is likely the explanation with regards to our previous results demonstrating that control of the magnitude of the net charge contained in a levitated droplet could be used to promote the cocrystallization CHCA with one or more peptides.[51] It should be noted that both cases of enhanced solute nucleation (i.e., single droplet vs population) involve ions$_{DNEC}$, albeit in different capacities, and hence both will be referred to as ion induced nucleation *in solution.*

NaCl usually occurs as cubic crystals, but other habits can be produced such as flake salt, which is obtained by careful surface evaporation of brine in flat pans open to the atmosphere. Dendritic salt is typically prepared by the evaporation of brine solutions that contain 5−20 ppm concentration of ferrocyanide ion, which suppresses growth on the crystal faces while enhancing growth at the crystal edges and corners.[102] While conducting the NaCl nucleation trials with droplet populations, it was observed that the NaCl crystal habit changed from regular, well formed, cubic shapes to dome-shaped dendrites as the induction potential used to impart charge on the droplets was increased.[52] As crystal habit is controlled by the kinetics of the atomic growth process through which assembly occurs,[3] we speculated that the change in droplet net charge (i.e., change in external growth conditions) was responsible for the observed dendritic $NaCl_{(s)}$. A set of experiments was then devised to better characterize this effect of ion-induced nucleation *in solution* on the observed NaCl crystal habit.

A calibrated 40 μm diameter orifice droplet dispenser with a 30 V applied waveform at 1 Hz was used to dispense droplets (initial volume = 260 $\pm$ 10 pL).[51] Four different starting solutions (1.1, 2.2, 3.3, or 4.4 mg of NaCl, 4, 8, 12, or 16 μL of glycerol, and 396, 392, 388, or 384 μL of dH_2O) were used to prepare droplet residue populations with similar $NaCl_{(aq)}$ concentrations, having initial droplet residue radii of 8.9, 11.2, 12.8, or 14.1 μm, respectively. For a given induction potential, a population of ∼40−70 droplets was dispensed and levitated for 5 min in the EDLT. The subsequent population of droplet residues was deposited onto a glass slide where each residue was then examined using optical microscopy.

The NaCl crystals, as formed within charged levitated droplets, had either regular, cube-like habits, or dome-shaped dendritic habits. The $NaCl_{(s)}$ dendrites formed were branched in one or more directions from a single point; each branch showing clear and distinguishable regions of curvature. Hence, we speculated that nucleation of dendrites also occurred in the diffuse layer at the droplet−air interface, and that crystal growth occurred along the droplet residue surface where mass transport at the liquid−gas interface was thought to be larger than that of the bulk solution.[103] Dendritic solute crystals with less defined shapes tend to form at higher supersaturations while crystals tend to be well formed at lower supersaturations in evaporating solution droplets.[98] Perhaps this is a type of surface-activated nucleation resulting in crystal formation (i.e., nucleation and crystal growth that occurs at the liquid−vapor interface) that has been thought to occur for ice in supercooled water droplets and for hydrates of nitric acid in concentrated nitric acid droplets,[104,105] although this can neither be confirmed nor disregarded based upon the theoretical and laboratory evidence available.[106] Recently, direct observation of surface-activated ice nucleation has been observed in undercooled sucrose solution droplets; however, none of the current theories for surface nucleation can properly describe the phenomenon.[107]

The percentage of dendritic $NaCl_{(s)}$ was plotted as a function of the induction potential for droplet residues of a particular radius (Figure 5A). The inflection point from each of the four trend lines plotted in Figure 5A was considered as the induction potential threshold necessary to incite a change in crystal habit for the nucleating $NaCl_{(s)}$. These threshold values are expressed in terms of surface charge density and are plotted as a function

(99) Kramer, B.; Hubner, O.; Vortisch, H.; Woste, L.; Leisner, T.; Schwell, M.; Ruhl, E.; Baumgartel, H. *J. Chem. Phys.* **1999**, *111*, 6521−6527.
(100) Svishchev, I. M.; Kusalik, P. G. *Phys. Rev. Lett.* **1994**, *73*, 975−978.
(101) Matsumoto, M.; Saito, S.; Ohmine, I. *Nature* **2002**, *416*, 409−413.
(102) Davidson, C. F.; Slabaugh, M. R. *J. Chem. Educ.* **2003**, *80*, 155−156.
(103) Hamai, M.; Mogi, I.; Tagami, M.; Awaji, S.; Watanabe, K.; Motokawa, M. *J. Cryst. Growth* **2000**, *209*, 1013−1017.
(104) Djikaev, Y. S.; Tabazadeh, A.; Reiss, H. *J. Chem. Phys.* **2003**, *118*, 6572−6581.
(105) Djikaev, Y. S.; Tabazadeh, A. *J. Phys. Chem. A* **2004**, *108*, 6513−6519.
(106) Kay, J. E.; Tsemekhman, V.; Larson, B.; Baker, M.; Swanson, B. *Atmos. Chem. Phys.* **2003**, *3*, 1439−1443.
(107) Hindmarsh, J. P.; Russell, A. B.; Chen, X. D. *J. Phys. Chem. C* **2007**, *111*, 5977−5981.

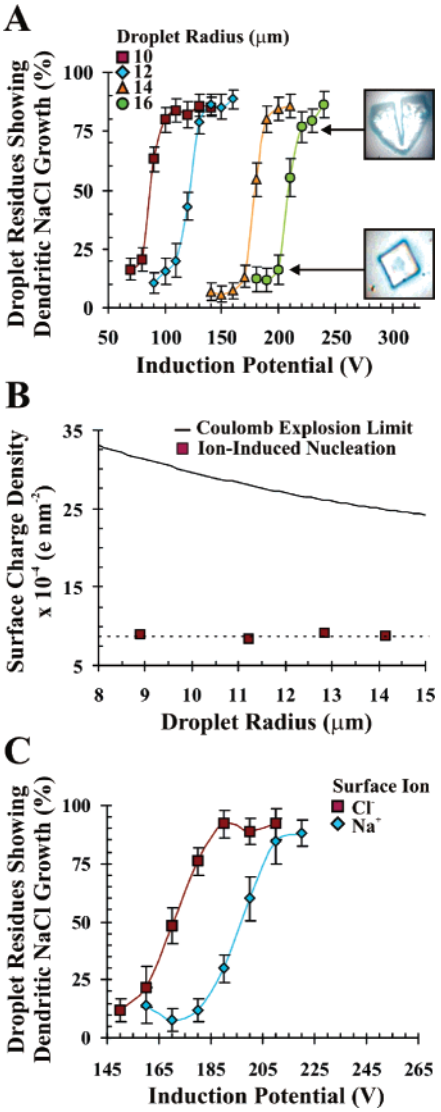

Figure 5. Change in NaCl crystal habit affected by variation of the change in the droplet residue populations. (A) Percent of droplet residues with dendritic NaCl precipitates as a function of induction potential (IP) for droplet residues of different radii. The two insets are representative images of NaCl crystals formed from droplet residues having a surface charge density below or above -9×10^{-4} e•nm^{-2} (bottom and top inset, respectively). (B) Surface charge density of levitated droplet residues as a function of the droplet radius showing the threshold necessary to induce NaCl dendrite formation, as indicated by the dotted line. The surface charge density at the theoretical Coulomb explosion limit for these droplet residues is indicated by the solid black line. (C) Percent of droplet residues with dendritic NaCl precipitates as a function of IP for droplet residues having different polarity of the net excess charge.

of the droplet residue radius (Figure 5B). As shown by the dotted line, dendritic NaCl crystal growth can be consistently observed once the droplet residue surface charge density surpasses a threshold of $\sim -9 \times 10^{-4}$ e•nm^{-2}. The surface charge density at the theoretical Coulomb explosion limit for these droplet residues was not reached in these trials, as indicated by the solid black line in Figure 5B. It should be noted that the presence of a growing crystal(s) in a droplet could affect the electric field and charge density in the droplet. This could occur if the growing crystal caused a change in the droplet's shape away from that of being a sphere, or if the growing crystal was charged. Molecular dynamic simulations are currently underway to investigate these scenarios.

Dome-shaped dendritic NaCl growth was not observed in experiments conducted with single quiescent droplets at a relative humidity between 0 and 5%. Thus, it is likely that the observed dendritic NaCl growth for droplet populations having higher net charge in the EDLT occurred because of an increase in droplet mobility which results in greater droplet deformation and higher rates of solvent evaporation as compared with droplet populations having a lower net excess charge, rather than the direct effect that excess ions$_{DNEC}$ may have on interfacial tensions (liquid−solid, vapor-solid, and vapor−liquid) within the droplet residues that favor surface-activated nucleation.[104] It should be noted that dendritic crystal growth usually occurs during faster rates of crystal growth whereby the excess energy of solidification at the solid interface is dissipated by convection (solution flow) rather than diffusion.

The effect of changing the net charge polarity of the droplets (i.e., changing the polarity of the induction electrode) on the observed NaCl crystal habit was determined. By changing the polarity of the induction electrode, the ions$_{DNEC}$ were switched from Cl^- to Na^+. A calibrated 40 μm diameter orifice droplet dispenser with a 30 V applied waveform at 1 Hz was used to dispense droplets (initial volume = 260 ± 10 pL).[51] By dispensing individually charged droplets directly onto a metal target plate connected to an electrometer, the magnitude of the droplet net charge for droplets of opposite polarity was measured to be identical within experimental error. A starting solution composed of 3.3 mg of NaCl, 12 μL of glycerol, and 388 μL of dH_2O was used to prepare initial glycerol droplet residues with radii of ~12.8 μm. A population of droplets was dispensed and levitated for 5 min in the EDLT, followed by droplet residue deposition and examination by optical microscopy. The procedure was repeated for various induction potentials of both polarities. The percentage of dendritic $NaCl_{(s)}$ was then plotted as a function of induction potential for droplet residues of different polarity (Figure 5C). The dendritic NaCl precipitates were observed for droplet residues with Cl^- ions$_{DNEC}$ at a lower induction potential threshold than observed for droplet residues with Na^+ ions$_{DNEC}$. Differences in the hydration spheres of Cl^- and Na^+ as well as the geometry and packing of the initial atomic cluster from which the nucleus grew could be factors for this result.[108,109] Recent computational and experimental studies have shown that in neutral aqueous solutions, Cl^- ions are present in the air/water interface at enhanced concentrations while Na^+ ions prefer the environment of the bulk liquid.[110] Thus, it was not surprising that nucleation occurred at a lower induction potential threshold for droplet residues with Cl^- ions$_{DNEC}$ than for droplet residues with Na^+ ions$_{DNEC}$, assuming that nucleation occurred at the droplet−air interface.

The effect of changing the solvent composition of the droplet residues on the observed NaCl crystal habit was determined. For the following trials, a calibrated 60 μm diameter orifice droplet dispenser with a 20 V applied waveform at 1 Hz was used to dispense a population of droplets (initial volume = 400 ± 20 pL). To ensure the levitated droplet residues were of similar size (residue diameter ~ 28 μm) and $NaCl_{(aq)}$ concentration, the composition of the starting solution used was systematically altered. Four different starting solutions (9.2, 11.5, 12.0, or 12.5 μL of glycerol, and 390.8, 388.5, 388.0, or 387.5 μL of

(108) Mucha, M.; Jungwirth, P. *J. Phys. Chem. B* **2003**, *107*, 8271−8274.
(109) Zahn, D. *Phys. Rev. Lett.* **2004**, *92*, 040801, 040801−040804.
(110) Garrett, B. C. *Science* **2004**, *303*, 1146−1147.

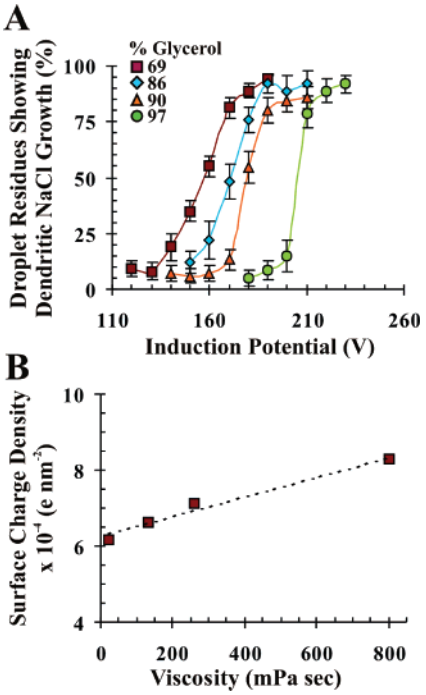

Figure 6. (A) Percent occurrence of dendritic NaCl crystals as a function of the induction potential for droplet residue populations having different water/glycerol solvent composition. (B) Surface charge density of levitated droplet residues as a function of droplet residue viscosity showing the threshold necessary to induce NaCl dendrite formation, as indicated by the dotted line.

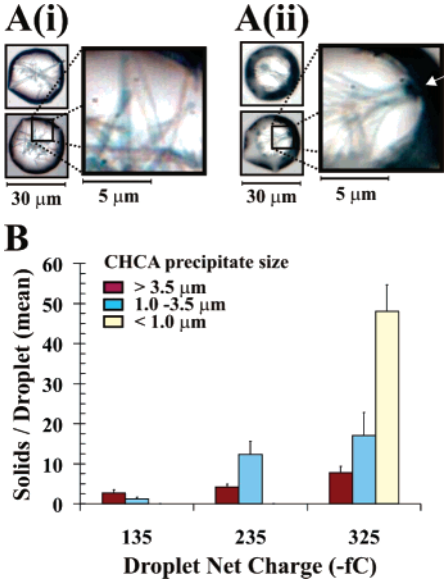

Figure 7. Representative images of crystals of (A (i, ii)) 2,4,6-trihydroxyacetophenone monohydrate (THAP) formed in levitated droplet residues having net excess charge of (i) −135 and (ii) −325 fC. (B) Size and number of CHCA precipitates formed in levitated droplet residues as a function of droplet net charge, precipitate diameter were >3.5 μm (red color), 1.0−3.5 μm (blue color), and <1.0 μm (cream color).

dH_2O), each containing 3.3 mg of NaCl, were used to dispense the initial droplets. By changing the relative humidity from 60% to 10% in the levitation chamber prior to the dispensing event, the percent glycerol in the droplet residues was varied from 68% to 97%.[81] As previously described, a population of droplets was dispensed and levitated for 5 min in the EDLT, followed by droplet residue deposition and examination by optical microscopy. The procedure was repeated using each solution at various induction potentials. The percentage of dendritic $NaCl_{(s)}$ was then plotted as a function of induction potential for droplet residues of different glycerol composition (Figure 6A). The results were similar to those presented in Figure 5A. Dendritic NaCl growth was consistently observed in droplet residues of various compositions once the induction potential reached a certain threshold. However in this case, the threshold was dependent on residue composition. There was a linear increase in the surface charge density required for dendritic NaCl growth over the range of viscosity sampled (Figure 6B). On the basis of these results, we suggest that surface ion_{DNEC} mobility is a factor in promoting NaCl dendrite formation.

Nucleation and Growth of THAP and CHCA in Levitated Droplets Having Net Charge. Increased magnitudes of droplet net excess charge also affected the nucleation and growth of two organic compounds, 2,4,6-trihydroxyacetophenone monohydrate (THAP) and α-cyano-4-hydroxycinnamic acid (CHCA), which have different crystal growth kinetics. Both compounds are commonly used as matrixes for MALDI, a laser-based soft ionization method whereby a sample is embedded in a chemical matrix that greatly facilitates the production of intact gas-phase ions from large, nonvolatile, and thermally labile compounds such as proteins, oligonucleotides, synthetic polymers, and high molecular weight inorganic compounds. The matrix plays a key role in this technique by absorbing the laser light energy and causing a small part of the target sample to vaporize and ionize.

For the following two preliminary trials, a calibrated 40 μm diameter orifice droplet dispenser with a 30 V applied waveform at 1 Hz was used to dispense droplet populations (initial volume = 260 ± 10 pL).[51] Each trial involved the nucleation and crystal growth of either 4.4 mg of THAP or 0.9 mg of CHCA dissolved in a mixed solvent (mixed solvent composition: 12 μL of glycerol, 40 μL of acetone, 50 μL of 0.1% trifluoroacetic acid (TFA) in dH_2O, 98 μL of dH_2O, and 200 μL of acetonitrile), one that we commonly employ during MALDI sample preparation.

In the first trial, which consisted of experiments with droplet populations containing THAP, the crystals that formed consisted of randomly stacked rods when the droplets had a net charge of −135 fC (Figure 7A(i)). When the droplets had a net charge of −325 fC, dendritic THAP crystals were observed in the population, as indicated by the dark branching points in Figure 7A(ii). Clear and distinguishable regions of crystal curvature were also observed, suggesting that nucleation occurred in the diffuse layer at the droplet−air interface, as indicated by the white arrow (inset, Figure 7A(ii)). As previously observed for NaCl solutions, dendritic growth occurred only under conditions of high net excess charge. Thus, we speculated that by varying the droplet net excess charge, dendritic THAP growth can be induced in each droplet of a levitated droplet population; a result of ion-induced nucleation *in solution*.

In the second trial, the net excess charge affected the number and size of observed CHCA precipitates (Figure 7B). By increasing the droplet net charge from −135 fC to −325 fC, there was a significant increase in the number of precipitates <1 μm in size from none to an average of 48.0 per droplet, respectively. Over the same increase in net charge, the relative abundance of precipitates >3.5 μm in size almost tripled from an average of 2.7 per droplet to an average of 7.8 per droplet, while the relative abundance of precipitates between 1.0 and

3.5 μm in size increased ~15 times from an average of 1.2 per droplet to an average of 17.0 per droplet. The observed increase in CHCA nucleation in these population trials for droplet residues having a high net charge is likely to have occurred because of the increased rate of solvent evaporation observed for a population of droplets having a high net charge, a result of ion-induced nucleation *in solution*.

The ability to influence CHCA precipitate size and number by changing the net excess charge of the droplets could be beneficial for MALDI sample preparation. Since MALDI is primarily based on laser desorption of solid analyte-matrix deposits (analyte:matrix = 1:1000), it suffers from the disadvantage of low reproducibility between laser shots. Decreasing crystal size increases crystal homogeneity and improves spot-to-spot reproducibility, minimizing the need to search for regions that yield maximal analyte signal-to-noise in the sample. Furthermore, the formation of smaller crystals has the advantage of smaller sample size and improved mass accuracy and resolution. Our previous studies have shown that peptide ion signal-to-noise ratios obtained by MALDI-MS from sample spots created from droplets that had high net excess charge were consistently greater than those detected from sample spots created from droplets that had low net excess charge.[51]

Nucleation and Growth of $NH_4NO_{3(s)}$ in Levitated Droplets Having Net Charge. A common constituent of atmospheric aerosols is ammonium nitrate, the vast majority of which is of anthropogenic origin.[111,112] Ammonium nitrate forms in the atmosphere when the hydroxyl radical oxidizes NO_x to nitric acid, which in the presence of ammonia, is neutralized to ammonium nitrate. In the absence of sunlight, nitric acid can be produced by the heterogeneous conversion of N_2O_5, formed from the reaction of NO_2 with NO_3, by hydrated aerosols.[112] Unlike most of the other hygroscopic salts that are found in the atmosphere, ammonium nitrate not only has a large efflorescence barrier[113−115] but has a relatively high vapor pressure. As such, ammonium nitrate has been the subject of a few rather limited studies of its hydration and dehydration properties. To this end, we demonstrate the use of ion-induced nucleation *in solution* to form ammonium nitrate particles from levitated droplets.

A calibrated 40 μm diameter orifice droplet dispenser with a 10 V applied waveform at 1 Hz was used to dispense single droplets from a 1.0 M NH_4NO_3 aqueous starting solution. Each single quiescent droplet was trapped and levitated for 5 min after which time the droplet residue was deposited onto a glass coverslip and examined with an optical microscope. Spherical polycrystalline $NH_4NO_{3(s)}$ particles were successfully formed at both low (−48 fC) and high (−110 fC) droplet net excess charge when the relative humidity of the EDLT chamber was kept below 31%. For % RH ≥ 31, only small droplets were observed, even when the levitation time was increased to 24 h for both low and high droplet net excess charges.

The efflorescence relative humidity (ERH) of 31% observed for NH_4NO_3 was similar to that reported by Chan et al. and within the range reported by Tang (ERH ~30%, and 25−32%, respectively).[116,117] In contrast, other groups have observed anhydrous NH_4NO_3 particles in a liquid-like state that fail to effloresce.[112,113,118,119] On the basis of their experiments with NH_4NO_3 particles that have been repeatedly cycled through deliquescence and efflorescence, Lighthouse et al. have confirmed the existence of anhydrous liquid NH_4NO_3 and have suggested that the wide range of efflorescent points previously reported was due to heterogeneous nucleation on unknown impurities present in every one of the water sources used, regardless of treatment.[112] Although these studies employed the use of an electrodynamic balance, the magnitudes of the droplet net excess charges used, along with droplet polarity, were not reported. We speculate that ion-induced nucleation *in solution* is also a factor that should be considered for the observed discrepancies in the NH_4NO_3 point of efflorescence since the highly supersaturated liquid-like state of NH_4NO_3 is reported to be very sensitive to foreign nuclei and to readily and reproducibly crystallize to the more stable crystalline anhydrous state in their presence.[112]

To this end, the effect of droplet net charge on NH_4NO_3 nucleation was also determined. A calibrated 40 μm diameter orifice droplet dispenser with a 10 V applied waveform at 1 Hz was used to dispense droplets from a 489 mM NH_4NO_3 aqueous starting solution containing 571 mM glycerol (water:glycerol = 97:3 v/v) into an EDLT chamber kept at a relative humidity (%RH) of 0−5%. The polarity of the induction electrode was set such that the identities of the $ions_{DNEC}$ that constitute the droplet net charge were NO_3^- $ions_{DNEC}$.

Two trials were conducted whereby single quiescent droplets containing NH_4NO_3 were dispensed, trapped, and levitated. Each droplet had either a net excess charge of ~−48 fC (induction potential (IP) = 130 V) or −110 fC (IP = 330 V), as previously described for single quiescent droplets containing NaCl. After 5 min of levitation, each quiescent single droplet residue was deposited onto a glass coverslip and the number of individual NH_4NO_3 crystals formed was counted. The crystals obtained in the droplet residues had regular bladed habits, and the area of each was measured in order to ascertain its size.

The results were plotted as histograms, as shown by the three representative examples (Figure 8). Each histogram consisted only of the data collected during one particular day since day-to-day differences in both room temperature and % RH (outside the levitation chamber where analysis of the droplet residues took place) were significant. Similar to the results obtained for NaCl containing single quiescent droplets, the histograms demonstrated that the size distribution and number of NH_4NO_3 crystals was affected by the net charge of the droplet. For droplet residues that had −48 fC net charge, the distribution of NH_4NO_3 crystals that had areas ≤50 μm^2 were 11.1, 14.3, and 20.4%, respectively, while the distribution of NH_4NO_3 crystals that had areas >125 μm^2 were 31.8, 31.2, and 32.3%, respectively. This distribution shifted toward smaller crystal size

(111) Finlayson-Pitts, B. J.; Pitts, J. N. *Chemistry of the Upper and Lower Atmosphere: Theory, Experiments, and Applications*; Academic Press: San Diego, CA, 2000.
(112) Lightstone, J. M.; Onasch, T. B.; Imre, D.; Oatis, S. *J. Phys. Chem. A* **2000**, *104*, 9337−9346.
(113) Dougle, P. G.; Veefkind, J. P.; ten Brink, H. M. *J. Aerosol Sci.* **1998**, *29*, 375−386.
(114) Doxsee, K. M.; Francis, P. E. *Ind. Eng. Chem. Res.* **2000**, *39*, 3493−3498.
(115) Hoffman, R. C.; Laskin, A.; Finlayson-Pitts, B. J. *J. Aerosol Sci.* **2004**, *35*, 869−887.
(116) Chan, C. K.; Flagan, R. C.; Seinfeld, J. H. *Atmos. Environ. Part A-Gen. Top.* **1992**, *26*, 1661−1673.
(117) Tang, I. N. *J. Geophys. Res.-Atmos.* **1996**, *101*, 19245−19250.
(118) Richardson, C. B.; Hightower, R. L. *Atmos. Environ.* **1987**, *21*, 971−975.
(119) Cziczo, D. J.; Abbatt, J. P. D. *J. Phys. Chem. A* **2000**, *104*, 2038−2047.

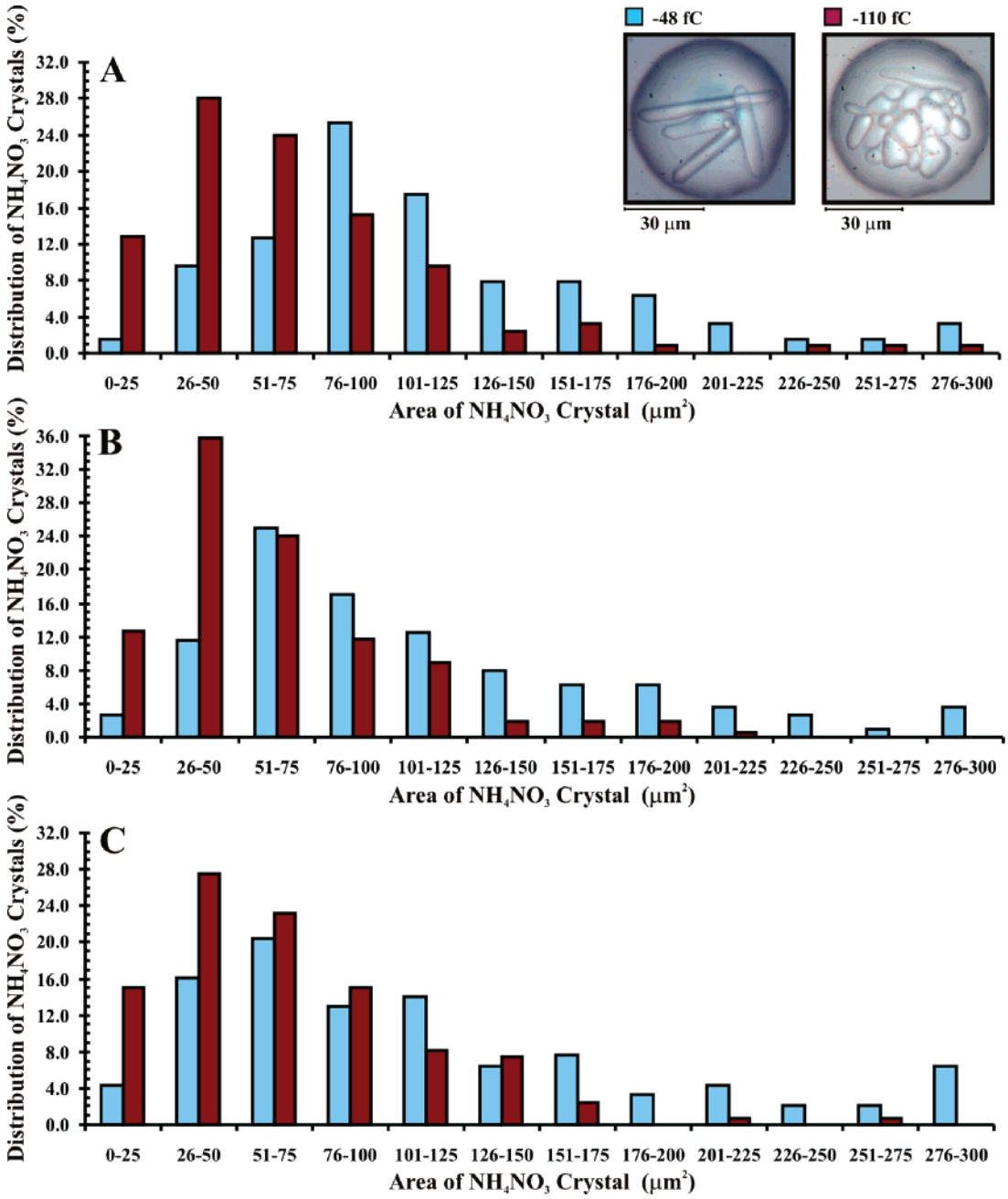

Figure 8. Size distribution of NH_4NO_3 crystals observed in single quiescent levitated droplet residues having a net excess charge of −48 fC (blue color) or −110 fC (red color), respectively over the course of 1 day. (A) Data collected on July 31st, 2006; ambient % RH = 33. (B) Data collected on August 1, 2006; ambient % RH = 38. (C) Data collected on August 2, 2006; ambient % RH = 43. The two insets are representative images of NH_4NO_3 crystals formed from single quiescent droplets having a net excess charge of −48 fC (left) or −110 fC (right), respectively.

as the droplet residue net charge increased to −110 fC (area ≤50 μm^2: 40.8, 48.5, and 42.5%, respectively; side length >125 μm^2: 8.8, 6.4, and 11.3%, respectively). Examination of the data also showed that the average number of crystals per droplet was almost doubled for droplets having higher net charge (−48 fC: number of crystals/droplet = 9.0, 10.2, and 8.5, respectively; −110 fC: number of crystals/droplet = 17.9, 17.0, and 14.5, respectively). This result suggested that increasing the magnitude of droplet net charge resulted in the promotion of solute nucleation for a given initial droplet residue NH_4NO_3 concentration. It is likely that the increase in the number of crystals present for droplets having higher net charge was responsible for the observed decrease in crystal size as a result of increased competition for solute molecules.

$NH_4NO_{3(s)}$ particle formation was also investigated for droplet populations under conditions of high relative humidity (i.e., % RH > 35). A calibrated 60 μm orifice droplet dispenser with a 50 V applied waveform at 120 Hz was used to dispense droplet populations from a 1 M aqueous solution of NH_4NO_3. The relative humidity of the EDLT chamber was ∼45%. In order to generate $NH_4NO_{3(s)}$ particles at this relative humidity, the temperature of the levitation chamber was elevated to 50 °C, at which point differences in the levitation time necessary for particle formation, dependent on the magnitude of the levitated droplet's net charge, were observed. The results are plotted in Figure 9.

An increase in IP from 150 to 500 V resulted in decreasing the induction time for $NH_4NO_{3(s)}$ formation from 30 min to 20 min. It should be noted that when charged droplets were

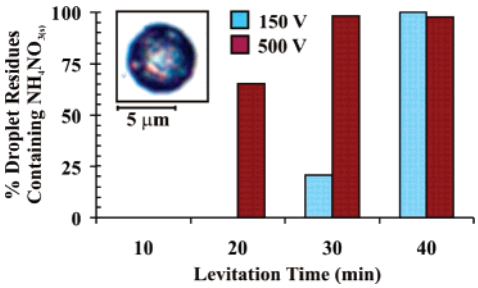

Figure 9. Percentage of droplet residues in which $NH_4NO_{3(s)}$ was observed for initial droplets having different net excess charge. IP = −150 V (blue color), IP = −500 V (red color), as a function of time. The inset is a representative image of an ammonium nitrate particle formed in the EDLT.

dispensed onto a sheet of Parafilm and placed in an incubator at the same relative humidity (45%) at 50 °C, no precipitation of $NH_4NO_{3(s)}$ was observed after 24 h. The $NH_4NO_{3(s)}$ particles will be utilized in our laboratory to perform dose−response trials to measure pro-inflammatory mediator differentiated expression by A549 cells, using the $NH_4NO_{3(s)}$ particles as a proxy for an ambient tropospheric particle type.[120]

Acknowledgment. This work was supported by funding from the National Science and Engineering Research Council of Canada (NSERC), Waters Technologies Inc., and Simon Fraser University. One of the authors (N.D.D.) is indebted to Dr. N. Weinberg for helpful discussions.

JA067094I

(120) Haddrell, A. E.; Ishii, H.; van Eeden, S. F.; Agnes, G. R. *Anal. Chem.* **2005**, *77*, 3623−3628.